

ReCLIP++: Learn to Rectify the Bias of CLIP for Unsupervised Semantic Segmentation

Jingyun Wang¹ and Guoliang Kang^{1*}

¹Beihang University, Beijing, China.

*Corresponding author(s). E-mail(s): kgl.prml@gmail.com;
Contributing authors: wangjingyun0730@gmail.com;

Abstract

Recent works utilize CLIP to perform the challenging unsupervised semantic segmentation task where only images without annotations are available. However, we observe that when adopting CLIP to such a pixel-level understanding task, unexpected bias (including class-preference bias and space-preference bias) occurs. Previous works don't explicitly model the bias, which largely constrains the segmentation performance. In this paper, we propose to explicitly model and rectify the bias existing in CLIP to facilitate the unsupervised semantic segmentation task. Specifically, we design a learnable "Reference" prompt to encode class-preference bias and a projection of the positional embedding in the vision transformer to encode space-preference bias respectively. To avoid interference, two kinds of biases are firstly independently encoded into different features, *i.e.*, the Reference feature and the positional feature. Via a matrix multiplication between the Reference feature and the positional feature, a bias logit map is generated to explicitly represent two kinds of biases. Then we rectify the logits of CLIP via a simple element-wise subtraction. To make the rectified results smoother and more contextual, we design a mask decoder which takes the feature of CLIP and the rectified logits as input and outputs a rectified segmentation mask with the help of Gumbel-Softmax operation. A contrastive loss based on the masked visual features and the text features of different classes is imposed, which makes the bias modeling and rectification process meaningful and effective. Extensive experiments on various benchmarks including PASCAL VOC, PASCAL Context, ADE20K, Cityscapes, and COCO Stuff demonstrate that our method performs favorably against previous state-of-the-arts. The implementation is available at: <https://github.com/dogehhh/ReCLIP>.

Keywords: Unsupervised semantic segmentation, CLIP, Bias rectification, Contrastive learning

1 Introduction

Semantic segmentation aims to attach a semantic label to each pixel of an image. Since the rise of deep learning [1–5], semantic segmentation has been widely adopted in real-world applications, *e.g.*, autonomous driving, medical image segmentation, *etc.* Conventional approaches [6–9] for semantic segmentation have achieved remarkable performance. However, the superior performance of those methods relies heavily

on large amounts of fully annotated masks. Collecting such high-quality pixel-level annotations can be both time-consuming and expensive, *e.g.*, some annotations for specialized tasks require massive expert knowledge, some are even inaccessible due to privacy reasons, *etc.* Therefore, it is necessary to explore unsupervised semantic segmentation where only images without annotations are available.

Unsupervised semantic segmentation (USS) has been studied for years. Many non-language-guided

USS methods have been proposed, *e.g.*, clustering-based methods [10–15], contrastive-learning-based methods [16, 17] and boundary-based methods [18], *etc.* Despite promising progress achieved, there still exhibits a large performance gap between USS and the supervised segmentation methods. Besides, these methods typically obtain class-agnostic masks and have to depend on additional processing (*e.g.*, Hungarian matching) to assign semantic labels to the masks, rendering them less practical in real scenarios.

Recently, large-scale visual-language pre-trained models, *e.g.*, CLIP [19], demonstrate superior zero-shot classification performance by comparing the degree of alignment between the image feature and text features of different categories. A few CLIP-based USS approaches [20–24] emerge and show remarkable performance improvement compared with the non-language-guided USS methods. These models require no access to any types of annotations, and can directly assign a label to each pixel, benefiting from the aligned vision and text embedding space of CLIP. However, good alignment between image-level visual feature and textual feature doesn't necessarily mean good alignment between pixel-level visual feature and textual feature. Thus, for CLIP, unexpected bias may inevitably appear. Previous works don't explicitly model such bias, which may largely constrain their segmentation performance.

When directly adopting CLIP in USS like MaskCLIP [20], we observe two kinds of biases existing in CLIP. From one aspect, as shown in Fig. 1 (a), CLIP exhibits space-preference bias. CLIP performs apparently better for segmenting central objects than the ones distributed near the image boundary. It can be reflected by the fact that mIoU decreases as the distance between the object centroid and the image centroid increases. From the other aspect, as shown in Fig. 1 (b), there exists class-preference bias between semantically relevant categories in CLIP. For example, according to visualizations (right), when the ground truth is a “sheep” (dark yellow), CLIP tends to incorrectly classify it as a “cow” (green). We also show such a trend between randomly selected classes by confusion matrix (left). Elements on the diagonal line represent the right classification, while others are false. We observe that besides ground truth, CLIP usually prefers to assign an incorrect but semantically relevant label to a pixel in quite a few cases, exhibiting a wide range of class-preference bias of CLIP.

In this paper, we propose to explicitly model and rectify the bias of CLIP to facilitate the USS. Specifically, we design two kinds of text inputs for each class, which are named “Query” and “Reference” respectively. The Query is manually designed and fixed while the Reference contains learnable prompts. We pass the Query and Reference through the text encoder of CLIP to obtain the Query feature and Reference feature. We adopt the Query feature as the segmentation head to generate the Query logits for each pixel of the image, which represents the original segmentation ability of vanilla CLIP. In contrast, we utilize the Reference feature to encode the class-preference bias. In addition, we project the positional embedding of CLIP's vision transformer to generate positional feature, which encodes the space-preference bias. The encoding processes of two biases are independent to avoid interference. Via a matrix multiplication between the Reference feature and the positional feature, a bias logit map is generated to explicitly represent two kinds of biases. Then, we remove the bias from the original CLIP via a logit-subtraction mechanism, *i.e.*, subtracting the bias logits from the Query logits. To make the rectified results smoother and more contextual, we concatenate the rectified logit map to the feature extracted by CLIP's visual encoder and pass them through a designed decoder. Then we apply the Gumbel-Softmax operation to the output of the decoder to generate a rectified mask. To make the bias modeling and rectification process meaningful and effective, the contrastive loss based on masked visual features (*i.e.*, applying rectified masks to the visual feature of CLIP and pooling) and text features of different categories is imposed.

We conduct extensive experiments on five standard semantic segmentation benchmarks, including PASCAL VOC [25], PASCAL Context [26], ADE20K [27], Cityscapes [28] and COCO Stuff [29]. Experiment results demonstrate that ReCLIP++ performs favorably against previous state-of-the-arts. Notably, on PASCAL VOC, our method outperforms MaskCLIP+ [20] by 15.4% and CLIP-S4 [23] by 13.4% mIoU. Extensive ablation studies verify the effectiveness of each design in our framework.

This paper is an extension of our conference paper [24]. To differentiate, we denote the method proposed in our conference version as ReCLIP and that in this paper as ReCLIP++. Compared to our conference version, we make further contributions, which are summarized as follows: 1) We optimize

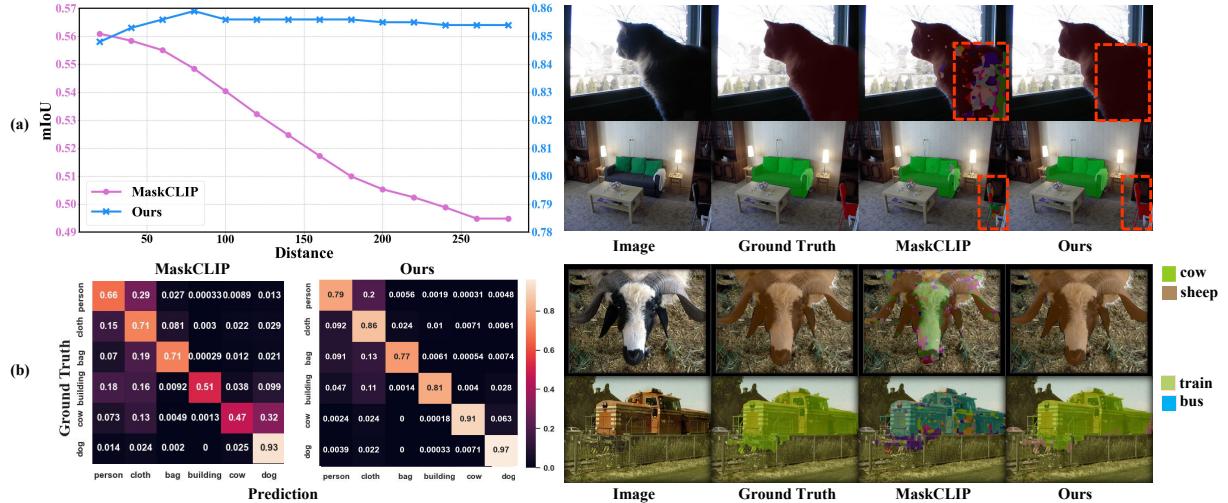


Fig. 1 (a) **Space-preference bias.** (Left): The relationship between distance (x -axis) and mIoU (y -axis) is drawn on PASCAL VOC [25]. The distance means the spatial distance between the object centroid and the image centroid and mIoU is computed based on predictions and ground truth. The curve shows that MaskCLIP [20] (pink) is apparently better at segmentation for central objects than boundary ones, but our method ReCLIP++ (blue) effectively mitigates this bias. More details about how we draw this figure have been shown in our appendix. (Right): Visualizations also show our improvement in space-preference bias qualitatively. (b) **Class-preference bias.** (Left): We randomly select 6 classes from PASCAL Context [26] and draw the confusion matrix of MaskCLIP and our model. It shows that besides the ground truth, MaskCLIP also prefers to assign an incorrect but semantically relevant label to a pixel in quite a few cases, while our results show an apparent improvement. (Right): The visualizations are consistent with what we observed in the confusion matrix. For example, for a “sheep” (dark yellow), MaskCLIP tends to classify it as a “cow” (green) incorrectly.

the design of the Bias Extraction Module. Specifically, we independently encode class-preference bias and space-preference bias into class-level Reference feature and patch-level positional feature respectively. Then the bias logit map, which explicitly represents both biases, is obtained by combining two features with matrix multiplication. 2) We additionally introduce a mask decoder, which takes the rectified logit map and the visual feature of CLIP as input and outputs smoother and more contextual rectified predictions. 3) We design a new strategy to generate a more accurate multi-label hypothesis for each image, which provides better supervision for the bias rectification process. 4) Benefiting from our new design, the distillation stage in ReCLIP is no longer necessary. We remove the distillation stage to simplify training and achieve even better segmentation performance. 5) We evaluate our methods on two more datasets including Cityscapes [28] and COCO Stuff [29]. On all the datasets, the segmentation performance of ReCLIP++ outperforms ReCLIP remarkably.

In a nutshell, our contributions are summarized as follows:

- We observe that when applying CLIP to pixel-level understanding tasks, unexpected biases, including

space-preference bias and class-preference bias, occur. These biases may largely constrain the segmentation performance of CLIP-based segmentation models.

- We propose to explicitly encode the class-preference and space-preference bias of CLIP via learnable Reference text inputs and projection of positional embedding respectively, and model both biases into one bias logit map via matrix multiplication. Through a simple logit-subtraction mechanism and the contrastive loss built on masked features of different classes, we effectively rectify the bias of CLIP.
- We conduct extensive experiments on segmentation benchmarks under the USS setting. Experiment results show superior performance of our method to previous state-of-the-arts.

2 Related Work

Pre-trained vision-language models. Pre-trained vision-language models (VLMs) [30–34] have developed rapidly with the help of large-scale image-text pairs available on the Internet. Recently, CLIP [19], ALIGN [35] and Slip [36] have made great progress

on learning visual and textual representations jointly by using contrastive learning. With the image-level alignment with text, pre-trained VLMs have a strong ability for zero-shot classification task and can be transferred to various downstream tasks, such as object detection [37, 38] and semantic segmentation [20, 39, 40].

Unsupervised semantic segmentation. While conventional approaches of semantic segmentation [6, 7] rely on pixel-level annotations and weakly-supervised methods [41–44] still ask for image-level labels, unsupervised semantic segmentation (USS) methods [11, 14, 16, 45, 46] explore to train a segmentation model without any annotations. Models like [47, 48] adopt generative model [49] to separate foreground with background or generate corresponding masks. SegSort [18], HSG[12] and ACSeg [15] use clustering strategy, while IIC [10] uses mutual information maximization to perform unsupervised learning. MaskContrast [16] introduces contrastive learning into USS. Others like DSM [13] and LNE [50] exploit features extracted from self-supervised models and spectral graph theory to facilitate segmentation. However, the methods mentioned above either fail to segment images with multi-category objects or show a large performance gap with the supervised methods. Besides, they can only obtain class-agnostic masks and have to depend on additional strategies, such as Hungarian-matching algorithm [51], to match the corresponding category with the segment. Recently, pre-trained vision-language models are adopted in USS. MaskCLIP [20] modifies the image encoder of CLIP to generate patch-level features and directly performs segmentation with text features as classifiers. CLIP-py [22] performs contrastive learning between visual features from self-supervised ViT [52] and text features from CLIP. ReCo [21] performs image retrieval with CLIP and extracts class-wise embedding as classifier with co-segmentation. CLIP-S4 [23] learns pixel embeddings with pixel-segment contrastive learning and aligns such embeddings with CLIP in terms of embedding and semantic consistency. These methods can directly assign a label to each pixel, which falls into the category of language-guided unsupervised semantic segmentation. However, directly applying CLIP in USS may result in unexpected bias. No previous method considers such bias. In this paper, we propose to explicitly model and rectify the bias of CLIP for unsupervised semantic segmentation.

Language-guided semantic segmentation. Recently, many works explore semantic segmentation guided

by language under different settings. Zero-shot works [53–56] split classes into seen and unseen sets. During the training period, only masks of seen classes are provided. For inference, models are tested on both seen and unseen classes, but the test data is still in the same distribution as the training data. Trainable open-vocabulary works [39, 40, 57–62] are trained in one scenario with extra annotations including class-agnostic masks or image captions but are used for predicting segmentation masks of novel classes in other scenarios. Recent training-free open-vocabulary works [20, 63, 64] adapt CLIP for semantic segmentation by modifying its architecture. These methods can directly perform inference on downstream datasets without any training. From the technical view, our method also falls into the category of language-guided semantic segmentation. However, we consider the unsupervised setting. In this setting, we have access to images without any annotations during training. The training and inference images are sampled from the same distributions and the same set of categories. Such a setting is different from the typical zero-shot or trainable open-vocabulary setting.

3 Method

Background In this work, we aim to rectify the bias of CLIP for unsupervised semantic segmentation. In USS, we only have access to images without any types of annotations to train the segmentation model. For training and inference, the same set of categories are considered and the data distributions are assumed to be the same.

Overview We aim to rectify the bias of CLIP including the class-preference bias and the space-preference bias, to facilitate unsupervised semantic segmentation. From a high level, class-preference bias reflects the shift of CLIP predictions towards specific classes, while space-preference bias reflects the shift of CLIP predictions towards specific spatial locations. Both biases will be finally reflected in the bias logit map. A reasonable way to rectify the bias is to subtract the bias logit map from the query logit map predicted by original CLIP.

The general framework of our method is illustrated in Fig. 2. We first forward the image $I \in \mathbb{R}^{3 \times H \times W}$ through the image encoder of CLIP to obtain the patch-level image feature Z . For each class, we manually design the text input which is named Query Q , and fix Q throughout the training. We pass Q through

the text encoder of CLIP to obtain query text feature W_q for each class, which serves as the weight of the query segmentation head. With W_q , we can obtain a query logit map M_q , which represents the segmentation ability of the original CLIP (Sec. 3.1).

We extract the bias existing in CLIP in a learnable way. Specifically, we design a kind of learnable text input named Reference R for each class. Passing R through the text encoder of CLIP, we obtain Reference text feature W_r , which is expected to encode the class-preference bias. Meanwhile, the positional embedding is projected into the positional feature W_p to encode the space-preference bias. Then the bias logit map M_b is extracted via a matrix multiplication between W_r and W_p (Sec. 3.2).

The Query logit map and the bias logit map are then passed through a Rectified Mask Generation module to generate rectified semantic masks. Firstly, a rectified logit map M is generated via a simple subtraction operation between M_q and M_b . Then, a mask decoder takes M and visual feature Z as input and outputs smoother and more contextual semantic masks with the help of Gumbel-Softmax operation (Sec. 3.3).

To enable a more meaningful and effective bias rectification, we generate a multi-label hypothesis for each image and impose contrastive loss based on masked visual features and Query text features of different classes (Sec. 3.4). CLIP is kept frozen during the training process.

3.1 Baseline: Directly Segment with CLIP

Following MaskCLIP [20], we adapt pre-trained CLIP [19] (ViT-B/16) to the semantic segmentation task. We remove the query and key embedding layers of last attention but reformulate the value embedding layer and the last linear projection layer into two respective 1×1 convolutional layers. Therefore, the image encoder can not only generate the patch-level visual feature for dense prediction but also keep the visual-language association in CLIP by freezing its pre-trained weights. We forward image I through the image encoder and obtain patch-level feature $Z \in \mathbb{R}^{n \times D}$ (n is the number of patches).

Each text Q_i in Query $Q = \{Q_1, Q_2, \dots, Q_C\}$ (C is the number of classes) is an ensembling of several manually designed templates, *e.g.*, “a good/large/bad photo of a [CLS]”, where [CLS] denotes a specific class name. Passing Q_i through the text encoder, we obtain different text embeddings for different manually designed templates. We average all those text

embeddings as the embedding of Q_i . Then the embeddings of all the Q_i in Q make up the query text feature $W_q \in \mathbb{R}^{C \times D}$. We treat text feature W_q as the weight of the segmentation head to perform 1×1 convolution. By sending feature Z to the segmentation head, we get a Query logit map $M_q \in \mathbb{R}^{n \times C}$. Then the segmentation mask can be predicted by arg max operation on M_q across the class channel C .

3.2 Bias Extraction

In the Bias Extraction Module, we aim to encode the class-preference bias and the space-preference bias of CLIP independently. Then we combine them into a bias logit map to explicitly model both biases.

Class-preference Bias Encoding. In order to encode the class-preference bias brought by pre-trained CLIP with respect to a specific segmentation task, we design learnable Reference text R_i in $R = \{R_1, R_2, \dots, R_C\}$ as an additional text input for each class. Inspired by CoOp [65], R_i consists of a learnable prompt which is shared across all the classes for efficiency, and a class name [CLS], which can be formed as

$$R_i = [v_1][v_2] \dots [v_l] \dots [v_L][CLS], \quad (1)$$

where each $[v_l]$ ($l \in \{1, \dots, L\}$) is a vector with dimension D and serves as a word embedding. The L is a constant representing the number of word embeddings to learn. Totally, there are 77 word embeddings for a textual input of CLIP. Among these, two word embeddings are used for representing class names and two for indicating the start and end of a textual input. Thus, we set L to 73.

Passing Reference R through the text encoder, we obtain reference text feature $W_r \in \mathbb{R}^{C \times D}$, which is expected to encode the class-preference bias. As Reference is only class-aware, the Reference feature is less likely to encode any space-related information.

Space-preference Bias Encoding. In ViT [66], positional embedding (PE) is important for encoding spatial information into features. Thus, we assume the space-preference bias should depend on the positional embedding (PE) and we choose to learn a projection of PE to encode the space-preference bias. The projection network of PE is designed as a 1-layer 1×1 convolutional network. Then we project PE p by the designed convolutional network to obtain positional feature $W_p \in \mathbb{R}^{n \times D}$. During the training process, the projection network is optimized to

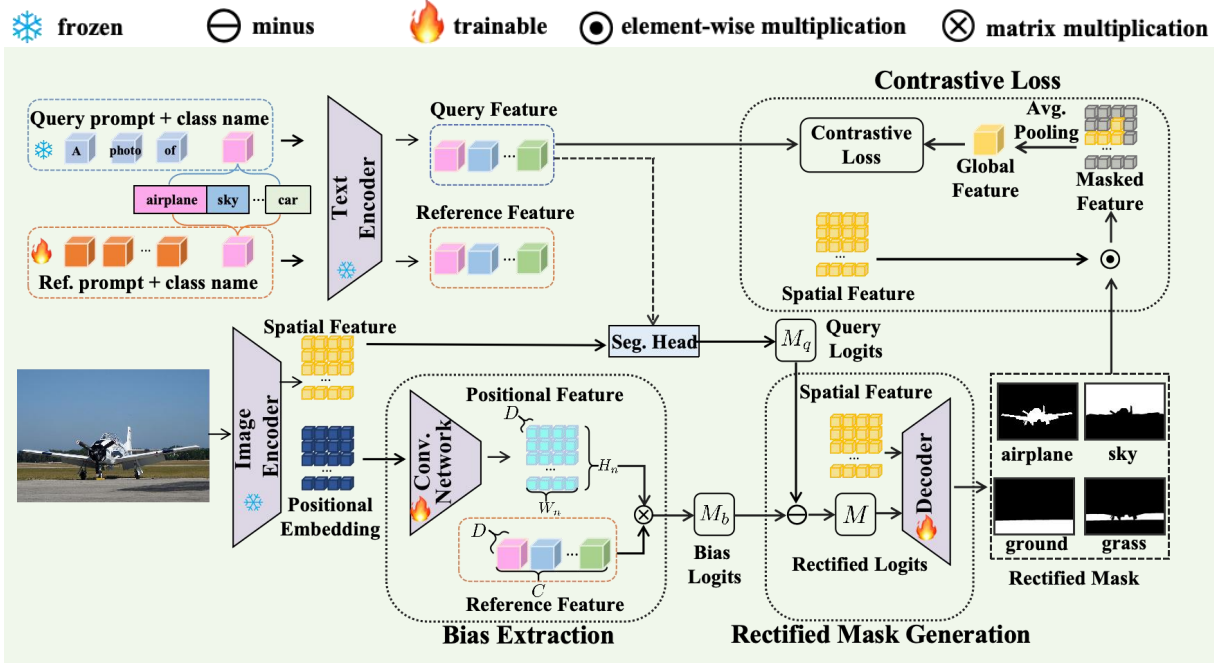


Fig. 2 Method overview of ReCLIP++. We propose a new framework for language-guided unsupervised semantic segmentation. We aim to rectify the class-preference and space-preference bias of CLIP via specifically designed Bias Extraction module, Rectified Mask Generation module, and Contrastive Loss module.

encode the space-preference bias with respect to each patch of the image. Note that the encoding process of space-preference bias is independent of that of class-preference bias because the encoding of space-preference bias doesn't rely on any class information.

Bias Logits Generation. With Reference feature W_r encoding the class-preference bias and positional feature W_p encoding the space-preference bias, we combine the encoding results of two biases to generate the final bias logit map $M_b \in \mathbb{R}^{n \times C}$, via a matrix multiplication as

$$M_b = W_p \times W_r^T. \quad (2)$$

Finally, M_b represents the final bias that we aim to remove from the predicted query logit map M_q of the original CLIP.

Bias Extraction: ReCLIP++ vs. ReCLIP. Note that the way of bias extraction in ReCLIP++ is different from that in ReCLIP [24]. In ReCLIP, to extract the class-preference bias, we compute the similarity between Reference features of different classes and CLIP's visual feature map Z to generate a class-preference bias logit map. However, as CLIP's image encoder takes PE as input to encode spatial

information into feature Z , the class-preference bias logit map may inevitably encode some space-related information. Consequently, the implicit space-related information in extracted class-preference bias may interfere with the extraction of space-preference bias, resulting in less effective bias extraction and rectification.

Differently, in ReCLIP++, we first encode class-preference bias and space-preference bias into the Reference feature and positional feature respectively. The reference feature only depends on class-related information (*i.e.*, learnable Reference text), while the positional feature only depends on space-related information (*i.e.*, PE). Thus, in this way, we may *independently* encode two kinds of biases and largely avoid the interference. As a result, with ReCLIP++, we realize more effective bias rectification and achieve better segmentation results (see Sec. 4 for more details).

3.3 Rectified Mask Generation

By keeping Query prompt Q fixed, the Query logit map M_q represents the natural prediction ability of the original CLIP model, which may contain class-preference bias and space-preference bias. With the

bias extraction module, we obtain M_b which represents the bias that we aim to remove from CLIP predictions. In this paper, we perform a simple element-wise subtraction between M_q and M_b to generate the rectified logit map M , *i.e.*,

$$M = M_q - M_b. \quad (3)$$

From a high level, this operation can be interpreted as subtracting the “bias” from the predictions with Query text feature W_q serving as the weight of the segmentation head.

Though the rectified logit map M can be directly used to generate semantic masks, the local context information is not considered, which may result in non-smooth mask predictions. Thus, different from our conference version [24], we additionally introduce a mask decoder \mathcal{F}_{dec} to transform M into a smoother and more contextual logit map. In our implementation, \mathcal{F}_{dec} consists of a convolutional layer with a 5×5 kernel and a batch normalization layer. We concatenate the rectified logit map M to the visual feature Z of CLIP and pass them through the mask decoder \mathcal{F}_{dec} to generate the rectified output $M_o \in \mathbb{R}^{n \times C}$, *i.e.*,

$$M_o = \mathcal{F}_{dec}(M, Z). \quad (4)$$

To generate the semantic mask $\hat{M} \in \mathbb{R}^{n \times C}$ for each category, a natural way is to employ arg max operation to M_o across the class channel C and generate the one-hot label for each spatial location. Then, each channel of \hat{M} corresponds to the mask for a specific category. However, as the arg max operation is not differentiable, we are not able to optimize \hat{M} end-to-end through gradient back-propagation during the training process. Thus we utilize a Gumbel-Softmax trick [67] to generate the semantic mask for each category with τ_1 as the temperature, *i.e.*,

$$\hat{M} = \text{Gumbel-Softmax}(M_o, \tau_1). \quad (5)$$

In this way, with our designed supervision (Sec. 3.4), the gradient can be back-propagated through \hat{M} to encourage a more effective bias rectification and a better semantic mask generation.

3.4 Bias Rectification via Contrastive Loss

In this section, we introduce a contrastive loss to supervise the rectification process.

Image-level multi-label hypothesis generation. In order to compute the contrastive loss, we need to know what classes exist in a specific image. However, this information is not available under the USS setting. In this section, we propose to generate an image-level multi-label hypothesis which means the set of classes that potentially exist in an image, to facilitate the following contrastive loss calculation.

In ReCLIP [24], we directly calculate the similarity scores between the class-level text features of manually designed prompts, *e.g.*, “a photo of a [CLS]”, and the image-level visual feature extracted by CLIP. We select the set of classes whose scores are higher than a threshold as the hypothesis. As CLIP is pre-trained to align image-level visual features with text features, it may focus on the most salient objects in an image and fail to recognize every existing object, rendering the multi-label hypothesis generated for ReCLIP less accurate.

In ReCLIP++, we design a new strategy to generate a more accurate multi-label hypothesis for an image. Given an image, we first split it into overlapped crops. Specifically, we slide a window across an image with a certain stride. In our implementation, we set the window width and height to r times the width and height of the input image and set the horizontal and vertical stride to half of the window width and height respectively. For each crop, we forward it through the visual encoder of CLIP to obtain its global visual feature and compute the similarity scores between the global visual feature and the Query feature W_q . We treat the class with the highest score as the detected class for this crop. Then for a given image, among all of its crops, we calculate the frequency $f(k)$ of the k -th class, $k \in \{1, 2, \dots, C\}$, being detected. We choose the classes with frequency higher than the threshold t as the multi-label hypothesis \mathcal{H} for an image, *i.e.*,

$$\mathcal{H} = \{k | k \in \{1, 2, \dots, C\} \text{ and } f(k) > t\}. \quad (6)$$

Bias Rectification via Contrastive Loss. We then design a contrastive loss to supervise the rectification process via aligning masked features with text features of corresponding classes. Specifically, we apply \hat{M} to the feature Z and perform a global average pooling to get the class-level masked features $Z_g \in \mathbb{R}^{C \times D}$, which encode the features of regions belonging to different classes. We compute the similarities between Z_g and text features of all the categories. As the masked features Z_g represent the objects of interest without context, we utilize W_q generated by text input

Q for similarity computation. With generated \mathcal{H} , the contrastive loss is computed as

$$\mathcal{L} = -\frac{1}{|\mathcal{H}|} \sum_{k \in \mathcal{H}} \log \frac{\exp\{S_{k,k}/\tau\}}{\sum_{j=1}^C \exp\{S_{k,j}/\tau\}} \quad (7)$$

where $S_{k,j}$ denotes the cosine similarity between visual feature of class $k \in \mathcal{H}$ and the text feature of j -th ($j \in \{1, 2, \dots, C\}$) category and the τ is a constant.

A better modeling of bias yields more accurate estimations of object masks. Then the masked features of objects are more aligned with the corresponding text features. As a result, the contrastive loss (Eq. (7)) will therefore be lower. In contrast, a worse modeling of bias results in higher contrastive loss. Thus, minimizing Eq. (7) will drive the model to update towards making more accurate mask predictions, *i.e.*, rectifying the bias of CLIP when adapting CLIP to the downstream USS task.

Note that in ReCLIP, an additional distillation stage is employed, where the knowledge of rectified CLIP is distilled into a specifically designed segmentation network like DeepLab-v2 [68]. However, in ReCLIP++, we don't need such a distillation stage. Empirically, we observe that such a distillation process has two opposing effects. On the one hand, it may benefit the smoothness of the predicated mask, which has a positive effect on the segmentation performance. On the other hand, instead of mitigating the bias, it may enlarge the bias to an extent, which has a negative effect on the segmentation performance. Benefiting from \mathcal{F}_{dec} , the rectified mask of ReCLIP++ is much smoother and contextual than that in ReCLIP, rendering the negative effect of distillation outweigh the positive effect of distillation. Thus, we choose not to employ the distillation in ReCLIP++ to make the training more simplified and achieve even better segmentation performance (see Sec. 4.4 for more details).

3.5 Inference

For the inference with ReCLIP++, we obtain the query logit map M_q by the query segmentation head and the bias logit map M_b which models both biases by the Bias Extraction Module. We then obtain the rectified output M_o by the Rectified Mask Generation Module with Eq. (4). With a simple arg max operation to M_o across the class channel C , we generate the rectified masks as final predictions.

4 Experiment

4.1 Setup

Datasets. We conduct experiments on five standard benchmarks for semantic segmentation, including PASCAL VOC 2012 [25], PASCAL Context [26], ADE20K [27], Cityscapes [28] and COCO Stuff [29]. PASCAL VOC 2012 (1,464/1,449 train/validation) contains 20 object classes, while PASCAL Context (4,998/5,105 train/validation) is an extension of PASCAL VOC 2010 and we consider 59 most common classes in our experiments. ADE20K (20,210/2,000 train/validation) is a segmentation dataset with various scenes and 150 most common categories are considered. Cityscapes (2,975/500 train/validation) consists of various urban scene images of 19 categories from 50 different cities. COCO Stuff (118,287/5,000 train/validation) has 171 low-level thing and stuff categories excluding background class. Following the previous evaluation protocol of unsupervised semantic segmentation methods [21, 46], we use 27 mid-level categories for training and inference.

Implementation details. For the image encoder of CLIP [19], we adopt ViT-B/16 as our visual backbone. For the text encoder of CLIP, we adopt Transformer [69]. During the whole training period, we keep both of the encoders frozen. We use conventional data augmentations including random cropping and random flipping. We use an SGD [70] optimizer with a learning rate of 0.01 and a weight decay of 0.0005. We adopt the poly strategy with the power of 0.9 as the learning rate schedule. We set $r = 1/6$ for all the datasets. We set $t = 7\%$ for PASCAL VOC and Cityscapes, and $t = 0$ for the rest datasets. In our experiment, we report the mean intersection over union (mIoU) as the evaluation metric. More details about training can be found in our appendix.

4.2 Comparison with previous SOTA

Baselines. We mainly compare our method with three types of semantic segmentation methods to verify the superiority of our method: (1) Trainable language-guided methods for OVSS task (TL-OVSS), including GroupViT [57], CoCu [62], and TCL [39]; (2) CLIP-based methods for training-free OVSS task (TF-OVSS), including CLIP [19] (vanilla CLIP visual encoder), MaskCLIP [20] (CLIP visual encoder with modified last-attention

block), SCLIP [64], and ClearCLIP [63]; (3) CLIP-based methods for USS task (C-USS), including MaskCLIP+ [20], CLIPPy [22], ReCo [21], CLIP-S4 [23] and ReCLIP [24]. We directly cite the corresponding results from the original papers, except that \dagger means the results are obtained by running the officially released source code and \ddagger means the results are cited from TCL [39]. All the numbers reported are presented as percentages. Among these, TL-OVSS methods rely on weak annotations like image-caption pairs to train the model, while TF-OVSS methods can directly perform open-vocabulary segmentation without any training. C-USS methods share the same language-guided unsupervised setting with ReCLIP++.

Comparison. The comparisons with previous state-of-the-art methods on five benchmarks are demonstrated in Table 1. From Table 1, we have the following observations: (1) C-USS methods consider the same setting as our method. We observe that ReCLIP++ outperforms previous state-of-the-art C-USS methods obviously, achieving new state-of-the-arts on all five benchmarks. Since ReCo [21] employs a “context elimination” (CE) trick which introduces prior knowledge to assist the training, we also report the results of ReCo by removing this trick (ReCo w/o. CE in Table 1) for a fair comparison. Notably, ReCLIP++ outperforms MaskCLIP+ by 15.4%, 5.0%, 4.2%, 1.3% and 4.3% respectively on the five datasets and outperforms CLIP-S4 by 13.4% and 2.5% on PASCAL VOC and PASCAL Context respectively. All these results verify the effectiveness of our ReCLIP++ in rectifying the bias of CLIP to assist unsupervised semantic segmentation (2) ReCLIP++ outperforms previous state-of-the-art TF-OVSS methods, implying that the bias of CLIP in complex visual understanding tasks cannot be fully rectified by simply modifying its architecture without any training. (3) TL-OVSS methods consider a different setting and are trained with large-scale image-caption pairs. Strictly speaking, our method cannot be directly compared with those works. However, the superior performance of ReCLIP++ compared to those typical TL-OVSS methods still demonstrates the effectiveness of ReCLIP++.

4.3 Comparison with Conference Version

In Table 2, we verify the effectiveness of each technical improvement of ReCLIP++ beyond the rectification stage of ReCLIP (rec.) [24] (our conference version): 1) we additionally introduce a decoder that

takes the rectified logit map and visual feature of CLIP as input and outputs smoother and more contextual masks (denoted as “Decoder”); 2) we design a new strategy to generate a more accurate label hypothesis for each image (denoted as “Label Hypothesis”); 3) we optimize the design of the bias encoding scheme to independently encode the class-preference and space-preference bias (denoted as “Independent”). In Table 2, we observe that when sequentially adding each technical component, the segmentation performance is consistently improved, which verifies the effectiveness of each technical contribution.

Finally, as shown in Table 1, with all these technical improvements, ReCLIP++ remarkably outperforms ReCLIP. Notably, we observe that even without a distillation, ReCLIP++ still outperforms ReCLIP on all benchmarks, which exhibits a stronger bias rectification capability of ReCLIP++ compared with ReCLIP. For example, on PASCAL VOC and Cityscapes, ReCLIP++ outperforms ReCLIP by 9.6% and 6.6% respectively.

4.4 Ablation study

Should Query be learnable? For text inputs Q and R , we only make Reference R learnable while keeping Query Q fixed. In this ablation, we study whether the prompt of Query should also be learnable. As shown in Table 3, we conduct experiments with learnable and fixed Query respectively. The numbers show that fixing Query obviously outperforms making Query learnable. The reason is when we make Query learnable, it may also implicitly capture bias, confusing the following bias rectification operations (e.g., bias logit subtraction). Therefore, in our framework, we choose to fix Q to make the bias rectification more effective.

Effect of element-wise subtraction on bias rectification. In order to validate the effect of our element-wise subtraction, we conduct experiments in Table 4. We compare our subtraction mechanism with an alternative solution: instead of subtracting the bias logit map M_b from the Query logit map M_q , we add M_b to M_q . Comparisons shown in the table verify the effectiveness of our subtraction way. As we aim to remove the bias from the original CLIP, we speculate that the subtraction operation may work as a strong prior which regularizes the training to facilitate meaningful and effective bias modeling.

Sensitivity to t and r in image-level multi-label hypothesis generation. When generating an image-level multi-label hypothesis as discussed in Sec. 3.4,

Table 1 Comparison with trainable language-guided methods for OVSS (TL-OVSS), CLIP-based methods for training-free OVSS (TF-OVSS), and CLIP-based methods for USS (C-USS) on five various benchmarks. \dagger means the results are obtained by running the officially released source code and \ddagger means the results are cited from TCL [39].

Method	Pub.	Setting	VOC	Context	ADE	City	Stuff
GroupViT [57] \ddagger	CVPR’22	TL-OVSS	79.7	23.4	9.2	11.1	15.3
TCL [39]	CVPR’23		77.5	30.3	14.9	23.1	19.6
CoCu [62]	NeurIPS’24		-	-	11.1	15.0	13.6
CLIP [19] \dagger	ICML’21	TF-OVSS	41.8	9.2	2.1	5.5	4.4
MaskCLIP [20]	ECCV’22		70.0 \dagger	21.7	12.2 \dagger	19.8 \dagger	13.6
SCLIP [64]	ECCV’24		76.9 \dagger	32.0	12.0 \dagger	15.3 \dagger	20.5
ClearCLIP [63] \dagger	ECCV’24		81.9	34.9	16.2	18.3	22.9
MaskCLIP+	ECCV’22	C-USS	70.0 \dagger	31.1	12.2 \dagger	25.2 \dagger	19.5 \dagger
CLIPPy [22]	ICCV’23		54.6	-	13.5	22.3	-
ReCo [21]	NeurIPS’22		55.2 \dagger	26.2	-	19.3	26.3
ReCo [21](w.o. CE) \dagger	NeurIPS’22		54.8	23.1	-	18.2	20.8
CLIP-S4 [23]	CVPR’23		72.0	33.6	-	-	-
ReCLIP (rec.) [24]	CVPR’24		58.5	25.8	11.1	16.2	14.6
ReCLIP [24]	CVPR’24		75.8	33.8	14.3	19.9	20.3
ReCLIP++	Ours		85.4	36.1	16.4	26.5	23.8

Table 2 Technical improvements of ReCLIP++ compared with ReCLIP. The first line is the results of ReCLIP after the rectification stage and the following lines are ablations experiments on the technical improvements of ReCLIP++ beyond ReCLIP. Results show that each newly added technical improvement of ReCLIP++ contributes to better results than ReCLIP.

ReCLIP (rec.)	+Decoder	+Label Hypothesis	+Independent	PASCAL VOC	PASCAL Context
✓				58.5	25.8
✓	✓			75.6	28.3
✓	✓	✓		77.3	31.4
✓	✓	✓	✓	85.4	36.1

Table 3 Ablation on whether Query should be learnable. The \times means fixed while \checkmark means learnable.

Query	Reference	VOC	Context	Cityscapes
✓	✓	11.6	3.6	2.3
\times	✓	85.4	36.1	26.5

t and r need to be determined. We study the sensitivity of our method to these hyper-parameters. As shown in Fig. 3, we observe that the mIoU of our method firstly increases and then decreases as t or r increases, exhibiting a typical bell curve. Such a curve shows the regularization effect of t and r on

Table 4 Effectiveness of element-wise subtraction. Results verify the effectiveness of our subtraction way.

Subtraction	Addition	VOC	Context	Cityscapes
\times	✓	77.7	33.3	21.5
✓	\times	85.4	36.1	26.5

the training. By replacing the multi-label hypothesis generation solution in ReCLIP++ with that used in ReCLIP (*i.e.*, “w/o. crop” in the figure), we obtain results that are inferior to ReCLIP++ within a vast range of t or r . All the results show that the solution

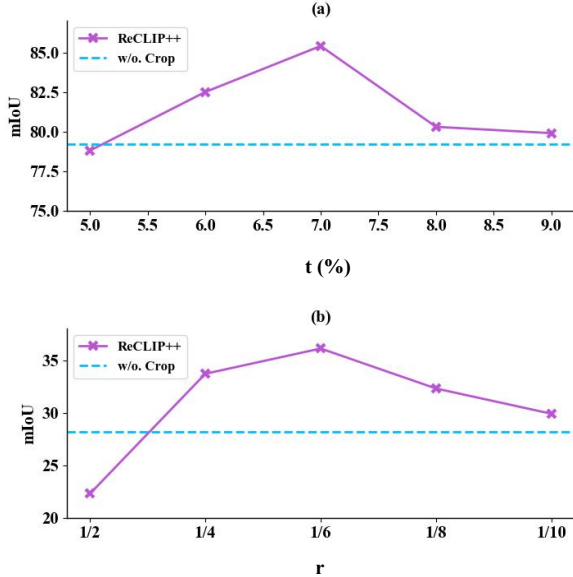


Fig. 3 Sensitivity to t and r in the image-level multi-label hypothesis generation. (a) Sensitivity to threshold t . (b) Sensitivity to r .

Table 5 Effect of Fine-tuning CLIP. The “Fine-tune CLIP” means we fine-tune the image encoder of CLIP.

Setting	VOC	Context	Cityscapes
Fine-tune CLIP	76.5	33.7	20.4
Frozen CLIP (Ours)	85.4	36.1	26.5

adopted in ReCLIP++ is insensitive to the choices of t and r and is superior to that used in ReCLIP.

Effect of Fine-tuning CLIP. We conduct experiments with fine-tuning the image encoder of CLIP in our framework. The results on PASCAL VOC, PASCAL Context, and Cityscapes are shown in Table 5. We find a consistent performance decrease compared with freezing CLIP. This is because fine-tuning CLIP on small-scale downstream datasets may harm the image-text alignment in pre-trained CLIP.

Effect of different bias rectification. We conduct experiments to evaluate how the rectification of each bias affects the segmentation performance in Table 6. Technically, when testing the rectification effect of the class-preference bias, we perform average pooling on the positional feature W_p along the spatial dimension and expand the pooling result to the original shape of W_p . Similarly, when testing the rectification effect of the space-preference bias, we perform average pooling

Table 6 Effectiveness of bias rectification. Results further verify that the rectification of both biases contributes to a better segmentation performance.

Class-preference	Space-preference	VOC	Context
✓	✗	76.4	34.1
✗	✓	76.6	32.4
✓	✓	85.4	36.1

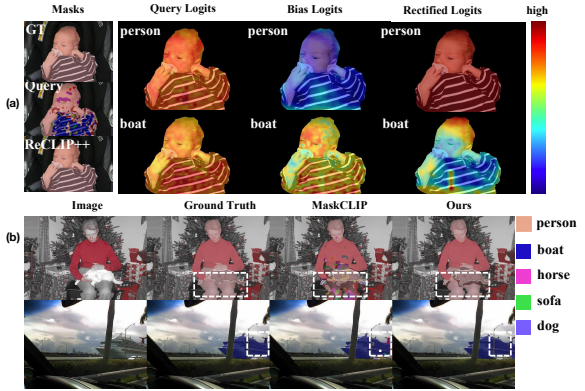


Fig. 4 Visualization of Bias Rectification. (a) **Class-preference bias:** In order to explain how the class-preference bias is explicitly encoded, we show the heatmap of the bias logit map. (b) **Space-preference bias:** The segmentation within dashed boxes shows the effectiveness of our method on rectifying space-preference bias.

on the reference text feature W_r along the class dimension and expand the pooling result to the original shape of W_r . Results on PASCAL VOC and PASCAL Context shown in Table 6 further verify that the rectification of each bias contributes to a better segmentation performance.

Bias Rectification Evaluation. In this ablation, we further evaluate the rectification effect of two biases both qualitatively and quantitatively.

(1) Qualitative evaluation of bias rectification. In Fig. 4 (a), we illustrate how we explicitly model and rectify the class-preference bias. As shown in the first column of Fig. 4 (a), the original CLIP (see “Query” mask) tends to misclassify part of a “person” (see the ground-truth mask denoted as “GT”) into a “boat”. Such a mistake is reflected in the comparison between the logit heatmaps for the “person” channel and the “boat” channel: in the area misclassified as “boat”, the logits for “boat” are relatively higher than those for “person”. In contrast, for the bias logit map, the person-channel logits are quite low, while the boat-channel logits are generally very high, especially for

the misclassified area. Consequently, via the proposed element-wise logit subtraction operation, we obtain the rectified logit map (see the last column), where the boat channel is largely suppressed. Finally, we obtain a much better mask (see “ReCLIP++” in the first column). In Fig. 4 (b), we aim to show that the space-preference bias is effectively modeled and rectified. By comparing the results of the original CLIP (see the dashed boxes of “Query” mask) and ReCLIP++ (see the dashed boxes of the last two columns), we find that the segmentation performance in the boundary areas is largely improved.

(2) Quantitative evaluation of bias rectification.

We further design two metrics to quantitatively evaluate the rectification results with respect to class-preference and space-preference bias respectively. For class-preference bias, we first compute the confusion matrix for all classes in the dataset. Given a class i , we take the i -th row of the confusion matrix. We perform a subtraction, between the i -th element and the maximum value among other positions of this row, as the score for class i . Then we average the scores for all classes. A higher average score reflects lower bias and better rectification results. For space-preference bias, we compute the slopes of the curve between the distance and mIoU at different distances (see Fig. 1 and Appendix for how to draw the curve) which roughly denote $\Delta \text{mIoU} / \Delta \text{Distance}$. We average the slopes at different distances. Obviously, a lower space-preference bias or a better rectification of space-preference bias should bring a higher score.

We show results on PASCAL Context for class-preference bias, and results on PASCAL VOC for space-preference bias, as there exhibits more obvious class-preference bias on PASCAL Context while more obvious space-preference bias on PASCAL VOC. According to results shown in Table 7, both ReCLIP (rec.) and ReCLIP++ can obviously rectify the class-preference and space-preference bias, compared with MaskCLIP which represents the original segmentation ability of CLIP. Compared with ReCLIP (rec.), ReCLIP++ exhibits stronger rectification results on both biases.

Why removing the distillation stage? As discussed in Sec. 3.4, in ReCLIP++, we don’t employ the distillation stage as adopted in ReCLIP. We observe that employing an additional distillation stage after ReCLIP++ leads to inferior results, as shown in Table 8. Further, we empirically study the effect of distillation on bias rectification. As shown in Table 7,

Table 7 Quantitative Evaluation of Bias Rectification. We design two metrics to evaluate the rectification effect on class-preference and space-preference bias respectively. Higher scores indicate lower bias or stronger rectification effect.

Method	Class-preference	Space-preference
MaskCLIP [20]	0.29	-0.50
MaskCLIP+ [20]	0.31	-0.48
ReCLIP (rec.) [24]	0.33	-0.41
ReCLIP++	0.40	0.05
ReCLIP++ & distill	0.37	-0.17

Table 8 Distillation results of ReCLIP++. Results show that distillation harms the segmentation performance.

Method	VOC	Context	ADE20K
ReCLIP++	85.4	36.1	16.4
Distillation	80.0	34.5	15.8

we observe that instead of mitigating the bias, further distillation after ReCLIP++ may enlarge the bias, which has a negative effect on the final segmentation performance. This phenomenon explains why the distillation stage is no longer necessary in ReCLIP++. In ReCLIP++, thanks to \mathcal{F}_{dec} , the rectified mask of ReCLIP++ is much smoother and contextual than that of ReCLIP, rendering the negative effect of distillation outweighs the positive effect of distillation and leading to a decrease of segmentation performance.

Qualitative Results. We visualize our segmentation results in Fig. 5. It can be observed that there exist apparent space-preference bias and class-preference bias in the segmentation results of the original CLIP (MaskCLIP). With ReCLIP, both biases can be partially removed. Moreover, ReCLIP++ exhibits stronger bias rectification capability compared with ReCLIP, yielding the best segmentation results.

5 Conclusion

In this paper, we propose a new framework for language-guided unsupervised semantic segmentation. We observe the bias, including space-preference bias and class-preference bias, exists in CLIP when directly applying CLIP to segmentation task. We propose using Reference text feature to encode class-preference bias and projecting positional embedding to encode space-preference bias independently, and then manage to combine them into a bias logit map



Fig. 5 Qualitative Results: We visualize segmentation results on both PASCAL VOC (left) and PASCAL Context (right). From the visualization, we observe that ReCLIP++ outperforms both MaskCLIP and ReCLIP obviously by rectifying both class-preference bias and space-preference bias.

by matrix multiplication. By a simple element-wise logit subtraction mechanism, we rectify the bias of CLIP. Then a contrastive loss is imposed to make the bias rectification meaningful and effective. Extensive experiments demonstrate that our method achieves superior segmentation performance compared with previous state-of-the-arts. We hope our work may inspire future research to investigate how to better adapt CLIP to complex visual understanding tasks.

References

- [1] G. Kang, Y. Wei, Y. Yang, Y. Zhuang, and A. Hauptmann, “Pixel-level cycle association: A new perspective for domain adaptive semantic segmentation,” *Advances in neural information processing systems*, vol. 33, pp. 3569–3580, 2020.
- [2] G. Kang, L. Jiang, Y. Wei, Y. Yang, and A. Hauptmann, “Contrastive adaptation network for single-and multi-source domain adaptation,” *IEEE transactions on pattern analysis and machine intelligence*, vol. 44, no. 4, pp. 1793–1804, 2020.
- [3] H. Shi, S. D. Dao, and J. Cai, “Llmformer: large language model for open-vocabulary semantic segmentation,” *International Journal of Computer Vision*, pp. 1–18, 2024.
- [4] Y. Yang, C. Ma, C. Ju, F. Zhang, J. Yao, Y. Zhang, and Y. Wang, “Multi-modal prototypes for open-world semantic segmentation,” *International Journal of Computer Vision*, pp. 1–17, 2024.
- [5] H. Wang, C. Yan, K. Chen, X. Jiang, X. Tang, Y. Hu, G. Kang, W. Xie, and E. Gavves, “Ov-vis: Open-vocabulary video instance segmentation,” *International Journal of Computer Vision*, pp. 1–18, 2024.
- [6] H. Zhao, J. Shi, X. Qi, X. Wang, and J. Jia, “Pyramid scene parsing network,” in *Proceedings of the IEEE conference on computer vision and pattern recognition*, 2017, pp. 2881–2890.
- [7] Q. Wang, B. Wu, P. Zhu, P. Li, W. Zuo, and Q. Hu, “Eca-net: Efficient channel attention for deep convolutional neural networks,” in *Proceedings of the IEEE/CVF conference on computer vision and pattern recognition*, 2020, pp. 11 534–11 542.
- [8] B. Cheng, A. Schwing, and A. Kirillov, “Per-pixel classification is not all you need for semantic segmentation,” *Advances in Neural Information Processing Systems*, vol. 34, pp. 17 864–17 875, 2021.
- [9] B. Cheng, I. Misra, A. G. Schwing, A. Kirillov, and R. Girdhar, “Masked-attention mask

transformer for universal image segmentation,” in *Proceedings of the IEEE/CVF Conference on Computer Vision and Pattern Recognition*, 2022, pp. 1290–1299.

[10] X. Ji, J. F. Henriques, and A. Vedaldi, “Invariant information clustering for unsupervised image classification and segmentation,” in *Proceedings of the IEEE/CVF International Conference on Computer Vision*, 2019, pp. 9865–9874.

[11] J. H. Cho, U. Mall, K. Bala, and B. Hariharan, “Picie: Unsupervised semantic segmentation using invariance and equivariance in clustering,” in *Proceedings of the IEEE/CVF Conference on Computer Vision and Pattern Recognition*, 2021, pp. 16 794–16 804.

[12] T.-W. Ke, J.-J. Hwang, Y. Guo, X. Wang, and S. X. Yu, “Unsupervised hierarchical semantic segmentation with multiview cosegmentation and clustering transformers,” in *Proceedings of the IEEE/CVF Conference on Computer Vision and Pattern Recognition*, 2022, pp. 2571–2581.

[13] L. Melas-Kyriazi, C. Rupprecht, I. Laina, and A. Vedaldi, “Deep spectral methods: A surprisingly strong baseline for unsupervised semantic segmentation and localization,” in *Proceedings of the IEEE/CVF Conference on Computer Vision and Pattern Recognition*, 2022, pp. 8364–8375.

[14] Y. Ouali, C. Hudelot, and M. Tami, “Autoregressive unsupervised image segmentation,” in *Computer Vision–ECCV 2020: 16th European Conference, Glasgow, UK, August 23–28, 2020, Proceedings, Part VII 16*. Springer, 2020, pp. 142–158.

[15] K. Li, Z. Wang, Z. Cheng, R. Yu, Y. Zhao, G. Song, C. Liu, L. Yuan, and J. Chen, “Acseg: Adaptive conceptualization for unsupervised semantic segmentation,” in *Proceedings of the IEEE/CVF Conference on Computer Vision and Pattern Recognition*, 2023, pp. 7162–7172.

[16] W. Van Gansbeke, S. Vandenhende, S. Georgoulis, and L. Van Gool, “Unsupervised semantic segmentation by contrasting object mask proposals,” in *Proceedings of the IEEE/CVF International Conference on Computer Vision*, 2021, pp. 10 052–10 062.

[17] K. He, H. Fan, Y. Wu, S. Xie, and R. Girshick, “Momentum contrast for unsupervised visual representation learning,” in *Proceedings of the IEEE/CVF conference on computer vision and pattern recognition*, 2020, pp. 9729–9738.

[18] J.-J. Hwang, S. X. Yu, J. Shi, M. D. Collins, T.-J. Yang, X. Zhang, and L.-C. Chen, “Segsort: Segmentation by discriminative sorting of segments,” in *Proceedings of the IEEE/CVF International Conference on Computer Vision*, 2019, pp. 7334–7344.

[19] A. Radford, J. W. Kim, C. Hallacy, A. Ramesh, G. Goh, S. Agarwal, G. Sastry, A. Askell, P. Mishkin, J. Clark *et al.*, “Learning transferable visual models from natural language supervision,” in *International conference on machine learning*. PMLR, 2021, pp. 8748–8763.

[20] C. Zhou, C. C. Loy, and B. Dai, “Extract free dense labels from clip,” in *Computer Vision–ECCV 2022: 17th European Conference, Tel Aviv, Israel, October 23–27, 2022, Proceedings, Part XXVIII*. Springer, 2022, pp. 696–712.

[21] G. Shin, W. Xie, and S. Albanie, “Reco: Retrieve and co-segment for zero-shot transfer,” *Advances in Neural Information Processing Systems*, vol. 35, pp. 33 754–33 767, 2022.

[22] K. Ranasinghe, B. McKinzie, S. Ravi, Y. Yang, A. Toshev, and J. Shlens, “Perceptual grouping in contrastive vision-language models,” in *Proceedings of the IEEE/CVF International Conference on Computer Vision*, 2023, pp. 5571–5584.

[23] W. He, S. Jamonnak, L. Gou, and L. Ren, “Clip-s4: Language-guided self-supervised semantic segmentation,” in *Proceedings of the IEEE/CVF Conference on Computer Vision and Pattern Recognition*, 2023, pp. 11 207–11 216.

[24] J. Wang and G. Kang, “Learn to rectify the bias of clip for unsupervised semantic segmentation,” in *Proceedings of the IEEE/CVF Conference on Computer Vision and Pattern Recognition*, 2024, pp. 4102–4112.

[25] M. Everingham, L. Van Gool, C. K. Williams, J. Winn, and A. Zisserman, “The pascal visual object classes (voc) challenge,” *International journal of computer vision*, vol. 88, pp. 303–338, 2010.

[26] R. Mottaghi, X. Chen, X. Liu, N.-G. Cho, S.-W. Lee, S. Fidler, R. Urtasun, and A. Yuille, “The role of context for object detection and semantic segmentation in the wild,” in *Proceedings of the IEEE conference on computer vision and pattern recognition*, 2014, pp. 891–898.

[27] B. Zhou, Z. Hang, F. X. P. Fernandez, S. Fidler, and A. Torralba, “Scene parsing through ade20k dataset,” in *2017 IEEE Conference on Computer Vision and Pattern Recognition (CVPR)*, 2017.

[28] M. Cordts, M. Omran, S. Ramos, T. Rehfeld, M. Enzweiler, R. Benenson, U. Franke, S. Roth, and B. Schiele, “The cityscapes dataset for semantic urban scene understanding,” in *Proceedings of the IEEE conference on computer vision and pattern recognition*, 2016, pp. 3213–3223.

[29] H. Caesar, J. Uijlings, and V. Ferrari, “Coco-stuff: Thing and stuff classes in context,” in *Proceedings of the IEEE conference on computer vision and pattern recognition*, 2018, pp. 1209–1218.

[30] Y.-C. Chen, L. Li, L. Yu, A. El Kholy, F. Ahmed, Z. Gan, Y. Cheng, and J. Liu, “Uniter: Universal image-text representation learning,” in *European Conference on Computer Vision*, 2020, pp. 104–120.

[31] K. Desai and J. Johnson, “Vortex: Learning visual representations from textual annotations,” in *Proceedings of the IEEE/CVF conference on computer vision and pattern recognition*, 2021, pp. 11 162–11 173.

[32] G. Li, N. Duan, Y. Fang, M. Gong, and D. Jiang, “Unicoder-vl: A universal encoder for vision and language by cross-modal pre-training,” in *Proceedings of the AAAI conference on artificial intelligence*, vol. 34, no. 07, 2020, pp. 11 336–11 344.

[33] J. Li, R. Selvaraju, A. Gotmare, S. Joty, C. Xiong, and S. C. H. Hoi, “Align before fuse: Vision and language representation learning with momentum distillation,” *Advances in neural information processing systems*, vol. 34, pp. 9694–9705, 2021.

[34] L. Li, Y.-C. Chen, Y. Cheng, Z. Gan, L. Yu, and J. Liu, “Hero: Hierarchical encoder for video+language omni-representation pre-training,” in *Proceedings of the 2020 Conference on Empirical Methods in Natural Language Processing (EMNLP)*, 2020, pp. 2046–2065.

[35] C. Jia, Y. Yang, Y. Xia, Y.-T. Chen, Z. Parekh, H. Pham, Q. Le, Y.-H. Sung, Z. Li, and T. Duerig, “Scaling up visual and vision-language representation learning with noisy text supervision,” in *International Conference on Machine Learning*. PMLR, 2021, pp. 4904–4916.

[36] N. Mu, A. Kirillov, D. Wagner, and S. Xie, “Slip: Self-supervision meets language-image pre-training,” in *European Conference on Computer Vision*. Springer, 2022, pp. 529–544.

[37] Y. Du, F. Wei, Z. Zhang, M. Shi, Y. Gao, and G. Li, “Learning to prompt for open-vocabulary object detection with vision-language model,” in *Proceedings of the IEEE/CVF Conference on Computer Vision and Pattern Recognition*, 2022, pp. 14 084–14 093.

[38] Z. Wang, Y. Li, X. Chen, S.-N. Lim, A. Torralba, H. Zhao, and S. Wang, “Detecting everything in the open world: Towards universal object detection,” *arXiv preprint arXiv:2303.11749*, 2023.

[39] J. Cha, J. Mun, and B. Roh, “Learning to generate text-grounded mask for open-world semantic segmentation from only image-text pairs,” in *Proceedings of the IEEE/CVF Conference on Computer Vision and Pattern Recognition*, 2023, pp. 11 165–11 174.

[40] M. Xu, Z. Zhang, F. Wei, H. Hu, and X. Bai, “Side adapter network for open-vocabulary semantic segmentation,” in *Proceedings of the IEEE/CVF Conference on Computer Vision and Pattern Recognition*, 2023, pp. 2945–2954.

[41] J. Ahn and S. Kwak, “Learning pixel-level semantic affinity with image-level supervision for weakly supervised semantic segmentation,” in *Proceedings of the IEEE conference on computer vision and pattern recognition*, 2018, pp. 4981–4990.

[42] Y. Du, Z. Fu, Q. Liu, and Y. Wang, “Weakly supervised semantic segmentation by pixel-to-prototype contrast,” in *Proceedings of the IEEE/CVF Conference on Computer Vision and Pattern Recognition*, 2022, pp. 4320–4329.

[43] P. O. Pinheiro and R. Collobert, “From image-level to pixel-level labeling with convolutional networks,” in *Proceedings of the IEEE conference on computer vision and pattern recognition*, 2015, pp. 1713–1721.

[44] J. Xie, J. Xiang, J. Chen, X. Hou, X. Zhao, and L. Shen, “C2am: contrastive learning of class-agnostic activation map for weakly supervised object localization and semantic segmentation,” in *Proceedings of the IEEE/CVF Conference on Computer Vision and Pattern Recognition*, 2022, pp. 989–998.

[45] W. Van Gansbeke, S. Vandenhende, S. Georgoulis, M. Proesmans, and L. Van Gool, “Scan: Learning to classify images without labels,” in *Computer Vision–ECCV 2020: 16th European Conference, Glasgow, UK, August 23–28, 2020, Proceedings, Part X*. Springer, 2020, pp. 268–285.

[46] M. Hamilton, Z. Zhang, B. Hariharan, N. Snavely, and W. T. Freeman, in *The Tenth International Conference on Learning Representations, ICLR 2022, Virtual Event, April 25-29, 2022*.

[47] A. Bielski and P. Favaro, “Emergence of object segmentation in perturbed generative models,” *Advances in Neural Information Processing Systems*, vol. 32, 2019.

[48] M. Chen, T. Artières, and L. Denoyer, “Unsupervised object segmentation by redrawing,” *Advances in neural information processing systems*, vol. 32, 2019.

[49] A. Creswell, T. White, V. Dumoulin, K. Arulkumaran, B. Sengupta, and A. A. Bharath, “Generative adversarial networks: An overview,” *IEEE Signal Processing Magazine*, vol. 35, no. 1, pp. 53–65, 2018.

[50] Z. Deng and Y. Luo, “Learning neural eigenfunctions for unsupervised semantic segmentation,” *arXiv preprint arXiv:2304.02841*, 2023.

[51] H. W. Kuhn, “The hungarian method for the assignment problem,” *Naval research logistics quarterly*, vol. 2, no. 1-2, pp. 83–97, 1955.

[52] M. Caron, H. Touvron, I. Misra, H. Jégou, J. Mairal, P. Bojanowski, and A. Joulin, “Emerging properties in self-supervised vision transformers,” in *Proceedings of the IEEE/CVF international conference on computer vision*, 2021, pp. 9650–9660.

[53] M. Bucher, T.-H. Vu, M. Cord, and P. Pérez, “Zero-shot semantic segmentation,” *Advances in Neural Information Processing Systems*, vol. 32, 2019.

[54] Y. Xian, S. Choudhury, Y. He, B. Schiele, and Z. Akata, “Semantic projection network for zero- and few-label semantic segmentation,” in *Proceedings of the IEEE/CVF Conference on Computer Vision and Pattern Recognition*, 2019, pp. 8256–8265.

[55] G. Pastore, F. Cermelli, Y. Xian, M. Mancini, Z. Akata, and B. Caputo, “A closer look at self-training for zero-label semantic segmentation,” in *Proceedings of the IEEE/CVF Conference on Computer Vision and Pattern Recognition*, 2021, pp. 2693–2702.

[56] B. Li, K. Q. Weinberger, S. J. Belongie, V. Koltun, and R. Ranftl, “Language-driven semantic segmentation,” in *The Tenth International Conference on Learning Representations, ICLR 2022, Virtual Event, April 25-29, 2022*.

[57] J. Xu, S. De Mello, S. Liu, W. Byeon, T. Breuel, J. Kautz, and X. Wang, “Groupvit: Semantic segmentation emerges from text supervision,” in *Proceedings of the IEEE/CVF Conference on Computer Vision and Pattern Recognition*, 2022,

pp. 18 134–18 144.

[58] G. Ghiasi, X. Gu, Y. Cui, and T.-Y. Lin, “Scaling open-vocabulary image segmentation with image-level labels,” in *Computer Vision–ECCV 2022: 17th European Conference, Tel Aviv, Israel, October 23–27, 2022, Proceedings, Part XXXVI*. Springer, 2022, pp. 540–557.

[59] J. Xu, J. Hou, Y. Zhang, R. Feng, Y. Wang, Y. Qiao, and W. Xie, “Learning open-vocabulary semantic segmentation models from natural language supervision,” in *Proceedings of the IEEE/CVF Conference on Computer Vision and Pattern Recognition*, 2023, pp. 2935–2944.

[60] P. Ren, C. Li, H. Xu, Y. Zhu, G. Wang, J. Liu, X. Chang, and X. Liang, “Viewco: Discovering text-supervised segmentation masks via multi-view semantic consistency,” *arXiv preprint arXiv:2302.10307*, 2023.

[61] F. Liang, B. Wu, X. Dai, K. Li, Y. Zhao, H. Zhang, P. Zhang, P. Vajda, and D. Marculescu, “Open-vocabulary semantic segmentation with mask-adapted clip,” in *Proceedings of the IEEE/CVF Conference on Computer Vision and Pattern Recognition*, 2023, pp. 7061–7070.

[62] Y. Xing, J. Kang, A. Xiao, J. Nie, L. Shao, and S. Lu, “Rewrite caption semantics: Bridging semantic gaps for language-supervised semantic segmentation,” *Advances in Neural Information Processing Systems*, vol. 36, 2024.

[63] M. Lan, C. Chen, Y. Ke, X. Wang, L. Feng, and W. Zhang, “Clearclip: Decomposing clip representations for dense vision-language inference,” *arXiv preprint arXiv:2407.12442*, 2024.

[64] F. Wang, J. Mei, and A. Yuille, “Sclip: Rethinking self-attention for dense vision-language inference,” in *European Conference on Computer Vision*. Springer, 2025, pp. 315–332.

[65] K. Zhou, J. Yang, C. C. Loy, and Z. Liu, “Learning to prompt for vision-language models,” *International Journal of Computer Vision*, vol. 130, no. 9, pp. 2337–2348, 2022.

[66] A. Dosovitskiy, L. Beyer, A. Kolesnikov, D. Weissenborn, X. Zhai, T. Unterthiner, M. Dehghani, M. Minderer, G. Heigold, and S. Gelly, “An image is worth 16x16 words: Transformers for image recognition at scale,” in *International Conference on Learning Representations*, 2021.

[67] E. Jang, S. Gu, and B. Poole, “Categorical reparameterization with gumbel-softmax,” in *5th International Conference on Learning Representations, ICLR 2017, Toulon, France, April 24-26, 2017, Conference Track Proceedings*, 2017.

[68] L.-C. Chen, G. Papandreou, I. Kokkinos, K. Murphy, and A. L. Yuille, “Deeplab: Semantic image segmentation with deep convolutional nets, atrous convolution, and fully connected crfs,” *IEEE transactions on pattern analysis and machine intelligence*, vol. 40, no. 4, pp. 834–848, 2018.

[69] A. Vaswani, N. Shazeer, N. Parmar, J. Uszkoreit, L. Jones, A. N. Gomez, Ł. Kaiser, and I. Polosukhin, “Attention is all you need,” *Advances in neural information processing systems*, vol. 30, 2017.

[70] H. Robbins and S. Monro, “A stochastic approximation method,” *The annals of mathematical statistics*, pp. 400–407, 1951.